Revisiting a stabilized landslide

Núria M. Pinyol[1,2], Mateu Maglia[1,2], Gaia Di Carluccio[2], Eduardo E. Alonso[1,2]

[1] Universitat Politècnica de Catalunya (UPC), Barcelona, Spain
[2] Centre Internacional de Mètodes Numèrics a l'Enginyeria (CIMNE), Barcelona, Spain

SUMMARY: This paper revisits a well-documented 5 million m^3 landslide identified in 1985 in the East of Spain in a reservoir flank that was induced by a quarry excavation of the toe and later stabilized by transferring mass from upper to lower levels. The landslide is still active and shows an extremely slow motion. The construction of a new pumping station for power generation will change the range and time variation of the reservoir level which will affect the slope stability. This paper first presents a stability back-analysis based on the material point method. The computed displacements induced by the excavation confirm the observed failure. Then, the current stability is evaluated based on in-situ measurements of pore water pressure. Finally, the assessment of the stability, including coupled hydro-mechanical analysis of the pore water pressure, based on finite element method, is carried out to evaluate the future stability.

Keywords: landslide, case history, numerical modelling, material point method

Introduction

A 5 million m^3 landslide was identified in 1985 close to the left abutment of a 116 m high arch-gravity dam in construction at that time. The measured displacement rates alarmed the people in charge of the dam project due to a potential sudden accelerated movement into the reservoir. They had in mind the case of the rapid landslide with catastrophic consequences in Vajont (Italy, 1963). At that time the causes explaining the sudden acceleration were uncertain.
After the geological and geotechnical characterization of the landslide, its stability was analysed, the triggering causes were identified, and stabilization measures were proposed and applied (Alonso et al. 1993). Based on field measurements, the landslide was described as the reactivation of an old translational landslide constituted by broken and pervious limestone strata overlaying a 2 m thick low permeability marl layer, which dips towards the reservoir (Fig. 1). No indications of water levels were found in any of the drilled boreholes. The sliding surface was localized into this clayey layer according to the inclinometer's measurements.

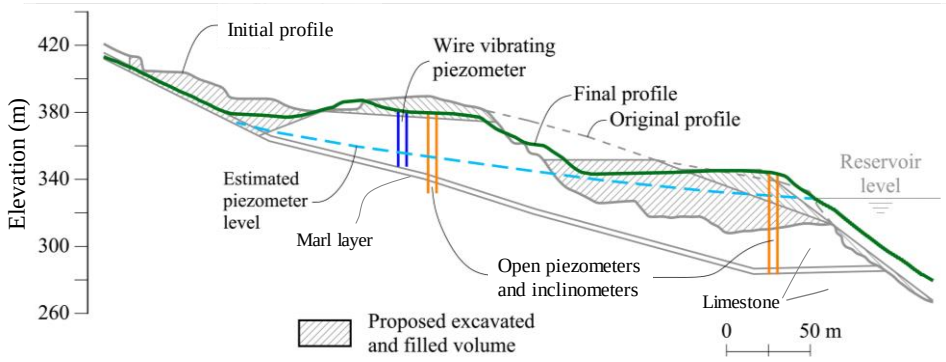

Figure 1. Representative section of the landslide

The quarry excavation of the landslide toe to provide granular aggregates for the concrete of the dam was identified as the triggering cause. Figure 1 shows the slope geometry before and after the quarry excavation. After evaluating several alternatives, the proposed measures to stabilize the slope consisted of excavating the upper part of the landslide and increasing the weight of the lower one. Figure 1 also includes the proposed geometry by Alonso et al. (1992) to stabilize the slope and the final geometry adopted.

The marl material was described as a low-plasticity clay ($w_L = 20 - 28\%$, $w_P = 13 - 14\%$) with high consistency ($w = 10 - 13.6\%$) and low porosity ($\phi = 0.25$). Block samples including the sliding surface were taken from the uncovered failure surface during the excavation works and tested in the direct shear apparatus. The sliding surface was aligned carefully with the middle plan of the shear box. The obtained frictional angle was 17-18º.

The back analysis and predictive stability analysis, after stabilization works, were carried out by Alonso et al. (1993) by means of a conventional limit equilibrium. They also presented a pioneering analysis of the internal distribution of stresses along the failure surface and the effect of loading and unloading sequences in the stabilization process through a finite element analysis with joint elements for the modelling of the failure surface. The stabilization works led to a decrease in the rate of movement, and the landslide was considered stabilized when the displacement rates remained non-relevant after the impoundment of the reservoir, which submerged the landslide toe, and two years of rainfall and reservoir level fluctuations.

The case is recovered in this paper and the landslide response is analysed with more recently developed numerical tools. The excavation process is simulated with a material point method-based analysis carried out with the open-source code Anura3D (Anura3D MPM Research Community, 2022). The accumulated displacement induced by the excavation is evaluated.

Almost 30 years later, the landslide, still instrumented with inclinometers and surface markers, as well as open and vibrating wire piezometers installed in the marl layer, remains active and exhibits an extremely slow motion (a few millimetres per year) (Fig. 2). The stability of the slope is analysed here under the established future variation of the water reservoir level due to the construction of a new pumping station for power generation.

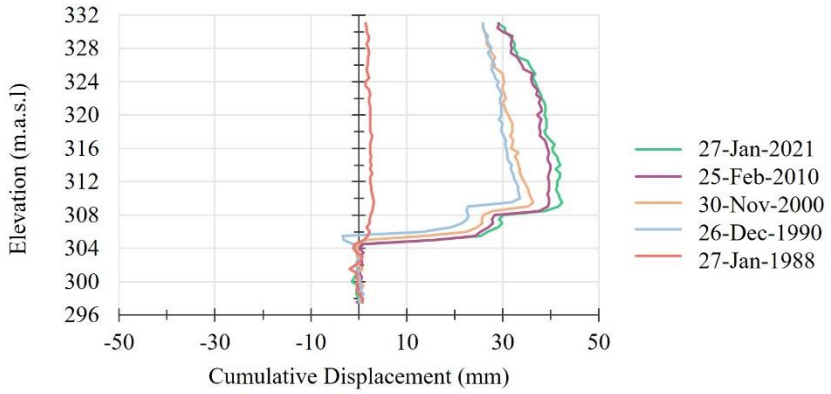

Figure 2. Inclinometer measurements

MPM modelling

The MPM (Sulsky et al., 1994) describes the continuum media with a set of Lagrangian material points that can move into a computational mesh that remains fixed through the calculation and covers the whole domain. A one-phase MPM analysis (Fern et al, 2019) is carried out to simulate the observed failure of the landslide induced by the excavation of part of the bank toe. No groundwater is included in the modelling according to Alonso et al. (1993).

Figure 3 shows the two materials considered and the domain discretization for the selected cross-section. Initially, four material points are defined per filled element.

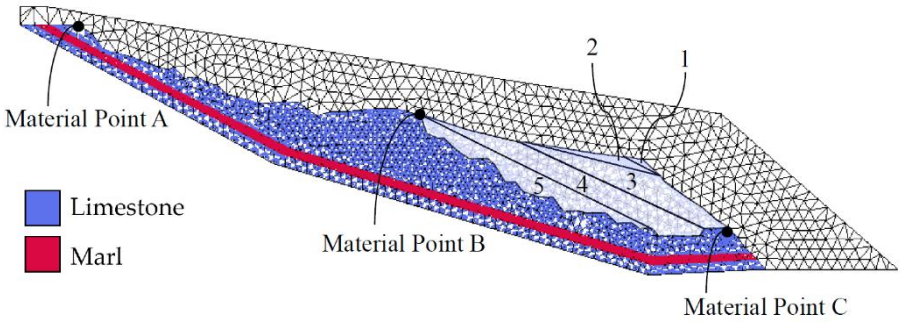

Figure 3. Materials, excavation volumes and computational mesh of 8,264 tetrahedral elements and 16,409 nodes.

The materials were characterized by a Mohr-Coulomb model with a linear elastic regime (Young's Modulus of 1000 and 200 MPa for limestone and marl, respectively, and Poisson's ratio of 0.33 for both). The limestone was defined as a brittle material with a strain-softening Mohr-Coulomb model in which the effective cohesion and effective friction angle drop from a peak to residual values as a function of the deviatoric plastic strain invariant, following an exponential law controlled by a "shape factor" parameter η:

$$c' = c'_r + (c'_p - c'_r)e^{-\eta\varepsilon_d^p}\,;\ \varphi' = \varphi'_r + (\varphi'_p - \varphi'_r)e^{-\eta\varepsilon_d^p}\,; \text{where } \varepsilon_d^p = \sqrt{\frac{2}{3}e_{ij}^p e_{ij}^p} \quad (1)$$

being e_{ij}^p the deviatoric component of the plastic strain tensor. Peak and residual values are indicated by the subindex p and r, respectively. Selected values are: c'_p=100 kPa, c'_r=20 kPa, φ'_p =35º, φ'_r=30º and η=500. Residual strength conditions (φ'_r=17.7º) were assigned to the marl layer.

The excavation of the volumes is simulated by instantaneously removing the material points of the volumes specified at the beginning of the calculation step. The total volume removed was divided into five subvolumes which are excavated subsequently (Fig. 3). Since no pore water pressure is included and the constitutive models are not time-dependent, the duration of the steps is not relevant. However, it is ensured that the slope is at rest before any subsequent excavation.

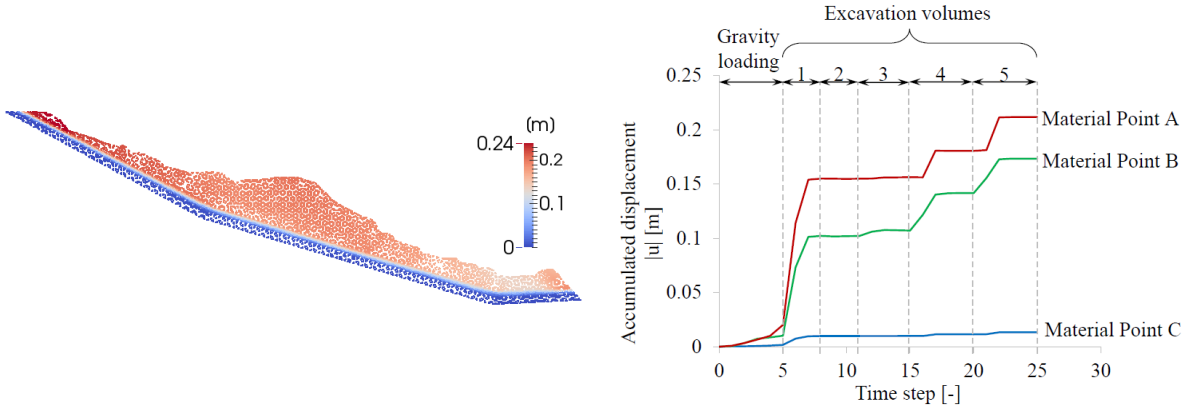

(a) (b)

Figure 4. (a) Total displacements at the end of calculation, after excavation. (b) Displacement versus time step of the three materials points indicated in Figure 3.

The calculation is divided into 7 stages. In the first stage, the initial stress distribution was estimated by a quasi-static stage in which the gravity loading is applied gradually and a local damping of 0.75 is applied. Afterwards, five stages were defined to simulate the excavation of the volumes (1 to 5) (Fig. 3). For these stages, the local damping is assigned equal to a low value of 0.05.

Figure 4 shows the computed displacements. The excavation process induces displacements of around 20 cm at the rock surface of the slope, resulting in a new equilibrium condition. The observed displacements are not homogeneous along the slope. A maximum accumulated displacement of 24 cm is computed in the upper part of the landslide, probably favoured by a local failure of the upper part due to the geometry of the cross-section. The minimum accumulated displacement calculated is located in the more stable portion of the slope's toe due to the shape of the marl layer. At each excavation stage, the accumulated displacement increases abruptly, and the motion is interrupted rapidly after a few centimetres once a new equilibrium is reached because of the evolution of geometry.

Analysis of actual state and future activities

The current stability of the landslide is evaluated taking into account the piezometric level estimated from operating open and wire vibrating piezometers (Fig. 1). The safety factor calculated is very close to 1, a fact that can explain the slow motion observed. The future stability is predicted by taking into account the pore water pressure distribution obtained from a numerical calculation carried out with the finite element method-based Code_Bright (Olivella et al., 2022) following the hydro-mechanical procedure presented in Pinyol et al. (2012). The evolution of the effective stress along the lower part of the sliding surface (Fig. 5) can be correlated with the variation of the safety factor. It is concluded that the slope will remain in very poor stability conditions with safety factors close to 1.

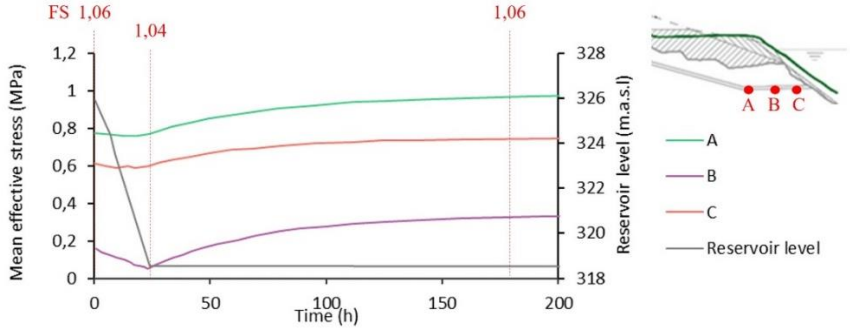

Figure 5. Effective stress in the three points plotted, reservoir level and the corresponding safety factor.

Conclusions

The stability of a well-documented landslide was reviewed by an MPM-based calculation procedure. The landslide reactivation may result in significant accumulated displacements but not in a catastrophic acceleration: the landslide moved downward in response to the excavation but it reached a new stable configuration at the expense of severe straining in the sliding surface and the rock cover. Analysing future stability requires the proper estimation of pore water pressure distribution induced by the established variation of the reservoir level.

References

Alonso EE, Gens A & Lloret A (1993). The landslide of Cortes de Pallas, Spain. *Géotechnique* 43(4), 507–521.

Anura3D MPM Research Community (2022) *Anura3D Version 2022 Source Code*. See http://www.anura3d.com

Fern EJ, Rohe A, Soga K, Alonso EE. (2019) *The Material Point Method for Geotechnical Engineering: A Practical Guide*. Editors, 271-286. CRC Press, 2019

Olivella S, Vaunat J & Rodríguez-Dono A. (2022). Code_Bright User's Guide. Version 9.

Pinyol NM, Alonso, EE, Corominas J & Moya J. (2012). Canelles landslide: modelling rapid drawdown and fast potential sliding. *Landslides* 9(1), 33–51.

Sulsky D, Chen Z & Schreyer HL (1994) A particle method for history-dependent materials. *Computer Methods in Applied Mechanics and Engineering*, 118(1–2), pp. 179–196.